International Journal of Air-Conditioning and Refrigeration
Vol. 28, No. 2 (2020) 2050018 (10 pages)

DOI: 10.1142/S2010132520500182

World Scientific
www.worldscientific.com

Experimental Investigation of Performance Enhancement of a Vapor Compression Refrigeration System by Vortex Tube Cooling

Phupoom Puangcharoenchai*, Pongsakorn Kachapongkun*,
Phadungsak Rattanadecho[†,‡,¶] and Ratthasak Prommas[*,§,¶]
*Rattanakosin College for Sustainable Energy and Environment
Rajamangala University of Technology Rattanakosin
Phutthamonthon, Nakhon Pathom 73170, Thailand
[†]Center of Excellence in Electromagnetic Energy
Utilization in Engineering (CEEE)
Department of Mechanical Engineering
Faculty of Engineering, Thammasat
University (Rangsit Campus)
Klong Luang, Pathumthani 12120, Thailand
[‡]ratphadu@engr.tu.ac.th
[§]ratthasak.pro@rmutr.ac.th

Received 12 January 2020
Accepted 30 March 2020
Published

This study aimed to analyze the difference in operation of the vapor compression refrigeration (VCR) system with vortex tube cooling. By using varied loads, experiments were conducted on the evaporator section of a vapor compression refrigeration system. In an attempt to improve the use of subcooling for the refrigeration, the effect of subcooling of refrigerant by vortex tube cooling was likewise examined. The test conditions included various loads (25%, 50%, 75% and 100%) and cold mass fractions (25%, 50% and 75%). This research described coefficient of performance (COP) as one of the significant parameters, in addition to heat rejection and refrigerating effect. The ideal efficiency appeared to be with the cold mass fraction of 25% and load of 100%, as identified by the results. Consequently, the COP could be enhanced by 5.16% along with an approximately 4.36% decline in average power use. Improved guidelines for vapor compression refrigeration systems to enhance the operation of the system are an expected benefit of this study.

Keywords: Coefficient of performance; subcooling; vortex tube.

Nomenclature

COP : Coefficient of performance
d : Cold-end orifice diameter (mm)
h : Enthalpy (kJ/kg)
q : Heat transfer (kJ/kg)
N : Inlet nozzle number
P : Pressure (bar)
ΔP : Pressure difference (bar)
T : Temperature (K)

¶Corresponding authors.

ΔT : Temperature difference (K)
D : Vortex tube diameter (mm)
L : Vortex tube length (mm)
w : Work required (kJ/kg)

Subscripts

c : Cold air/condenser
comp : Compressor
cond : Condenser
evap : Evaporator
h : Hot air
i : Inlet
IHE : Internal heat exchanger
o : Outlet
sat : Saturated
sub : Subcooled

1. Introduction

In terms of refrigeration, the operation of a vapor compression refrigeration (VCR) system can be enhanced using subcooling. Sometimes, this is done using a vortex tube, which is a small powered device used in cooling systems[1] discovered by Ranque, a French physicist, in 1933 (Ref. 2) and improved by the French Engineer Hilsch in 1947.[3] The device (shown in Fig. 1) is a basic one and comprises no moving parts. Using high-speed air compression, when high-pressure air flows through the nozzle hole in contact with the vortex tube surface, it creates hot and cold air simultaneously. A strong vortex inside the pipe and the splitting of hot and cold air apart are the result. The air is cooled in the center compared to the entrance, while the air around the pipe wall is hotter than the air at the entrance. Due to cold and hot air being separated, the cool air in the middle will flow through the hole facing the flow control valve, while hot air around the pipe wall will move within the valve to manage the flow.[4–6]

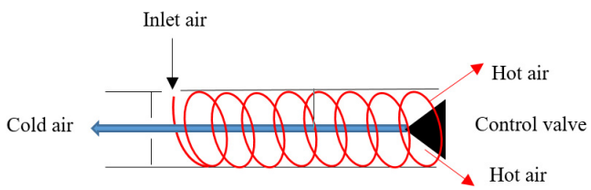

Fig. 1. Schematic of the counter-flow vortex tube with flow direction.[1]

The temperature separation in the vortex tube can be impacted by various factors, including geometrical controls and thermophysical features. Vortex tube length, vortex tube diameter, the diameter of the orifice, number and shape of the nozzles and the shape of the hot air outlet are the geometrical qualities. Air pressure at the inlet and gas type are the thermophysical properties. The effects of orifice nozzle number and the inlet pressure on the heating and cooling operations when air and oxygen are used as fluids were previously detailed by Kirmaci.[7] The temperature gradient is lowered with more orifice nozzles, as found by an experimental study. A helical swirl flow generator was created by Markal *et al.*[8] The effect of valve angle on the operation varies based on the value of L/D and it is found that valve angle has a weak effect on system performance. Different numbers of nozzles ($N = 1$–4) and inlet pressures ($P_i = 2$–3 bar) were used by Eiamsa-ard[9] for testing. An increase in nozzle number and supply pressure causes increased vortex intensity and energy separation in the tube, as shown by the results.

To moderate losses due to expansion and increase the coefficient of performance (COP) of the vapor compression refrigeration system,[10] subcooling of liquids before the isenthalpic expansion device can help. Including internal heat exchangers,[11,12] condenser subcooling[13] evaporative condensers[14] and thermoelectric peltier cooling module.[15]

Subcooling prior to the expansion process with an internal heat exchanger is shown in Fig. 2. Due to the enthalpy in the evaporator entrance decreasing and increasing in specific compression work, the internal heat exchanger will boost the refrigerating

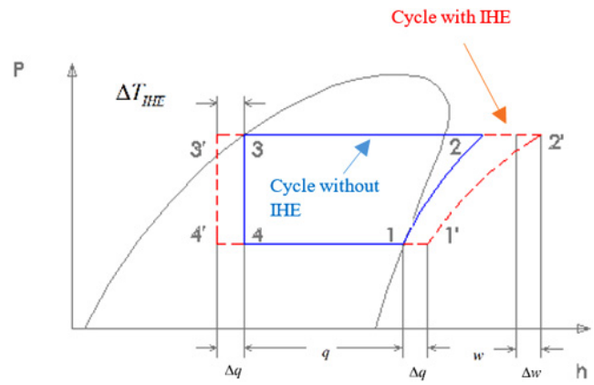

Fig. 2. Similarities concerning the theoretical cycles, with and without an internal heat exchanger, in the P–h diagram.[12]

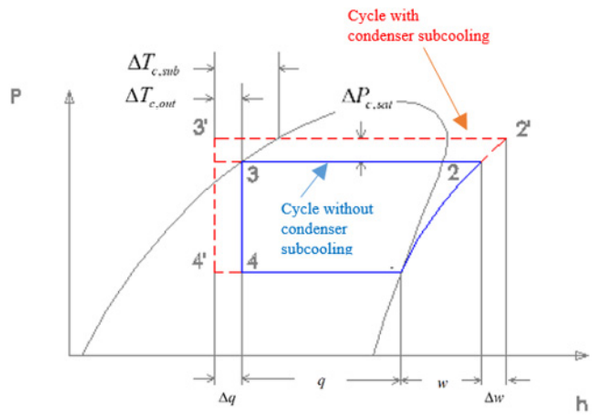

Fig. 3. Similarities concerning the theoretical cycles, with and without condenser subcooling, in the P–h diagram.[12]

effect because of the increased enthalpy of the superheated vapor at the compressor entrance.[16–20]

Condenser subcooling can boost the COP due to the reduction of the temperature at the outlet of the condenser (by $\Delta T_{c,\ sub}$) and the impact of adding specific work due to compression and because of the enhancement in condensing pressure (by $\Delta P_{c,\ sat}$), as shown in Fig. 3.[12]

One way to increase subcooling directly is by reducing the condensing pressure. Accordingly, the improvement of performance for the vapor compression refrigeration system by using cold air from the vortex tube is studied in this paper.

2. Methodology

Figure 4 illustrates the vapor compression refrigeration system using vortex tube cooling. First, the shutter valve is opened and an air flow meter is used to gauge the amount of compressed air. Afterwards, the air pressure is regulated by a pressure regulator before it goes into the vortex tube control. The compacted air that is discharged from the vortex tube is partitioned into different portions. The cool air portion moves through the wind current meter for quantification, at that point, into the heat exchanger to exchange heat from the refrigerant of the refrigeration framework, and finally, is released into the atmosphere. Conversely, hot air goes from the

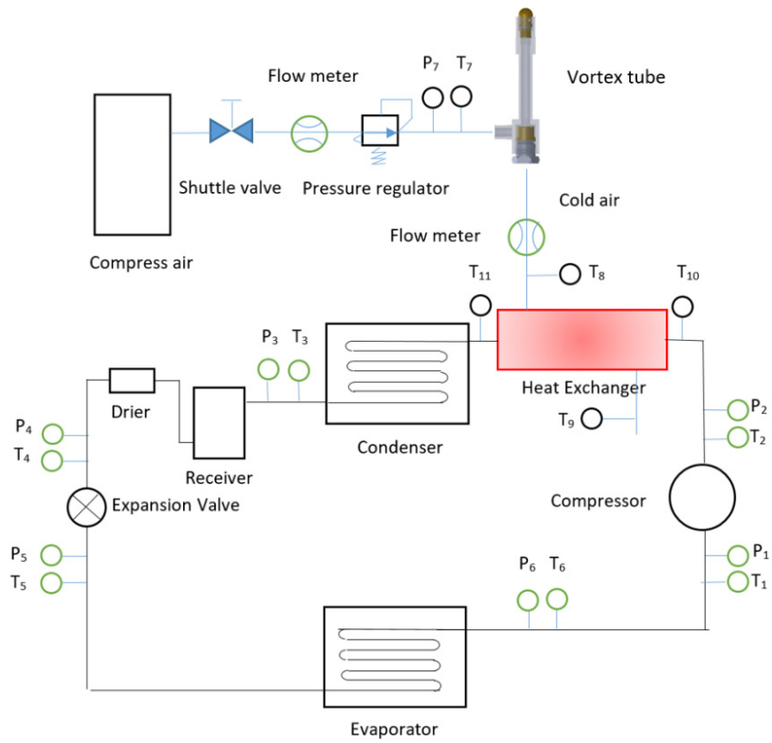

Fig. 4. Representation of the vapor compression refrigeration system using vortex tube cooling.

vortex tube into the valve for regulation, after which it is expelled back into the atmosphere.

2.1. *Experimental setup*

The experimental setup comprises a hermetically sealed reciprocating compressor, air-cooled condenser, receiver, drier, thermostatic expansion valve and the evaporator that is made of copper pipe with diameter and length of the tube being 9.5 mm (3/8 inch) and 7 m, respectively, which is installed in a hot water tank ($30 \times 30 \times 30\,cm^3$). The vortex tube and concentric heat exchanger are installed at the outlet of the compressor in the VCR system with a cooling capacity of 3000 BTU/h as shown in Fig. 5.

The heat loads will use a tubular heater (1.0 kW) as a heat source for the VCR system. This hot water will be used instead of the cooling load for the system. The heat loads can be controlled by adjusting the output voltage (0–250 V) through a variable-voltage transformer (TDGc2-1kVA) to control the heat loads at 25%, 50%, 75% and 100% as required.

For assessing high and low pressures, including the subcooled and superheated temperatures, digital manifold gauges (HVAC-Bluetooth model Testo-550) were used. The experimental uncertainties of measurement are as follows: pressure (low-side) ± 0.3 bar, temperature (subcooled) $\pm 0.5°C$, pressure (high-side) ± 0.3 bar and temperature (superheated) $\pm 0.5°C$. The compressor was operated by a clamp-on power logger model PW3360-21. Active power is $\pm 0.3\%$ rdg.

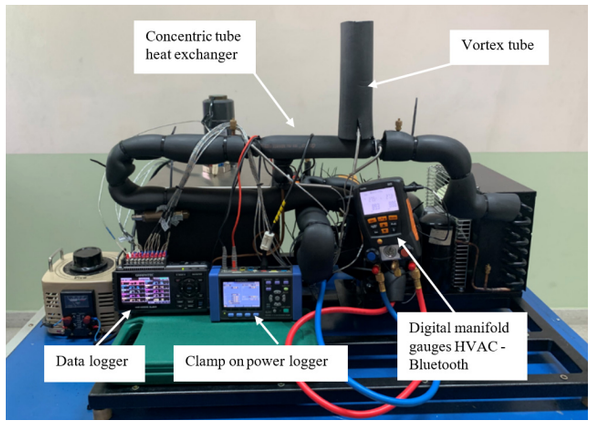

Fig. 5. Test setup of vapor compression refrigeration system using cold air from vortex tube cooling.

Turning on the refrigerator to assess various heat loads at 25%, 50%, 75% and 100% was the initial step in the experiment, after which the compressed air was released at a pressure of 2.0 bar using the flow meter. To manage the mass ratio of cold air to compressed air at the inlet (cold mass ratio), also called the cold mass fraction, the hot air control valve was varied at the vortex tube at 25%, 50% and 75%. Subsequently, the data was recorded every minute for 60 min for pressure, temperature, electric power, etc. Afterwards, identifying the heat rejection, refrigerating effect and coefficient of performance is done by calculating and comparing the results, such as by using electrical power in the system for refrigeration before enhancement.

2.2. *Vortex tube*

Cold mass fraction is defined as the ratio of cold air exit to the air entry mass flow rate. This is an important variable used to identify the performance of vortex tubes.

The counter-flow vortex tube has the following: length of a hot tube (L_h) is $4.5D$ and length of a cold tube (L_c) is $2.0D$. Based on previous works,[21–27] we have considered D as the inner diameter of the tube (12 mm). As can be seen in Fig. 6, the cold-end orifice diameter (d) is 6 mm, while the nozzle inlet is a six-way spray.

The operating pressure is 2 bar and the volume flow rate is $0.00125\,m^3/s$ (75 L/min). The cold mass fraction of 25% has the maximum temperature reduction of 20°C, followed by the cold mass fraction of 50%, where the temperature reduction to 13°C, and finally, the cold mass fraction of 75%, where the temperature reduction is 8°C.

2.3. *Concentric tube heat exchanger*

The vortex tube was planned to employ cold air to cool the discharge refrigerant pipe using a concentric

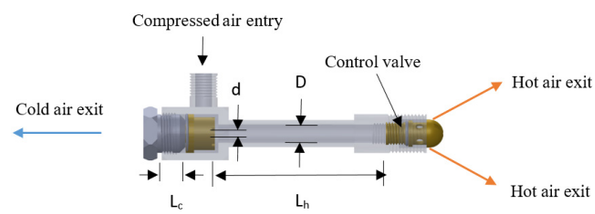

Fig. 6. Counter-flow vortex tube.

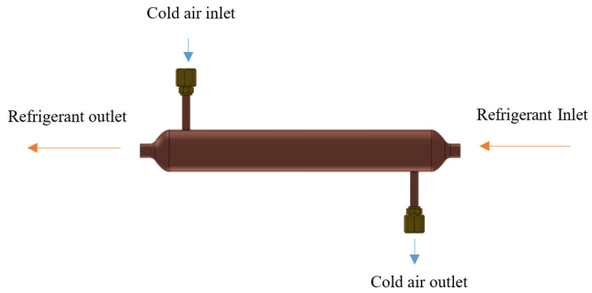

Fig. 7. Concentric tube heat exchanger.

tube heat exchanger.[28–35] As can be seen in Fig. 7, the inner tube is 10 mm in diameter and 200-mm long, while the outer annulus is 20 mm.

2.4. *Calculations using certain equations*

Equations (1)–(4) are used to test the coefficient of performance for the vapor compression refrigeration system with vortex tube cooling.

Equation (1) can be used to compute heat rejection:

$$q_{\text{cond}} = (h_{\text{cond},o} - h_{\text{cond},i}). \tag{1}$$

Equation (2) can be used to estimate the refrigerating effect:

$$q_{\text{evap}} = (h_{\text{evap},o} - h_{\text{evap},i}). \tag{2}$$

Equation (3) can be used to estimate the work required:

$$w_{\text{comp}} = (h_{\text{comp},o} - h_{\text{comp},i}). \tag{3}$$

Equation (4) can be used to assess the coefficient of performance:

$$\text{COP} = \frac{q_{\text{evap}}}{w_{\text{comp}}}. \tag{4}$$

3. Results and Discussion

This study details an operating refrigerator unit using the vapor compression refrigeration system and vortex tube cooling to improve the cooling of refrigerant at a high temperature by concentric tube heat exchangers before it enters the condenser. Heat rejection, refrigerating effect, work required and coefficient of performance for the refrigeration system can be resolved by gauging pressure, temperature and power use. In contrast, optimal conditions are demonstrated by the results from a refrigerator before and after the update with modified loads (25%, 50%, 75% and 100%) and separate cold mass fractions (25%, 50% and 75%).

3.1. *Comparison of heat rejection for the vapor compression refrigeration system*

Figure 8 shows the relationships between heat rejections at different loads (25%, 50%, 75% and 100%) and different cold mass fractions (25%, 50% and 75%). Equation (1) can be used to acquire these values. Heat rejection at 25% load is the highest, followed by those at 50%, 75% and 100% loads, as shown by the results.

Heat rejection at the load of 25% [Fig. 8(a)] had the highest value, followed by those at loads of 50% [Fig. 8(b)], 75% [Fig. 8(c)] and 100% [Fig. 8(d)], as shown by the results. It seems apparent that the increasing trend will have similar features, meaning the cold mass fraction of 25% has the highest value, followed by those of 50% and 75%, respectively. The cold mass fraction of 25% has the maximum heat rejection of 241.02 kJ/kg, followed by the cold mass fraction of 50%. Figure 8(a) shows that the heat rejection rose to 240.31 kJ/kg for a cold mass fraction of 75%, whereas the heat rejection rose to 240.19 kJ/kg for conventional systems. Further, the cold mass fraction of 25% has the highest heat rejection of 231.97 kJ/kg, for a load of 100% [as shown in Fig. 8(d)], followed by the cold mass fraction of 50%, where the heat rejection rose to 231.94 kJ/kg, and then the cold mass fraction of 75%, for which the heat rejection rose to 231.02 kJ/kg compared with conventional systems. This aids in the reduction of heat rejection in the condenser.

3.2. *Evaluation of refrigerating effect by the vapor compression refrigeration system*

Equation (2) can be used to determine the refrigerating effects (as shown in Fig. 9) against diverse loads (25%, 50%, 75% and 100%) and various cold mass fractions (25%, 50% and 75%).

The refrigerating effect at 25% load shows the maximum value, followed by those at 50%, 75% and 100% loads, respectively, as revealed by the results. In comparison to conventional systems, it seems

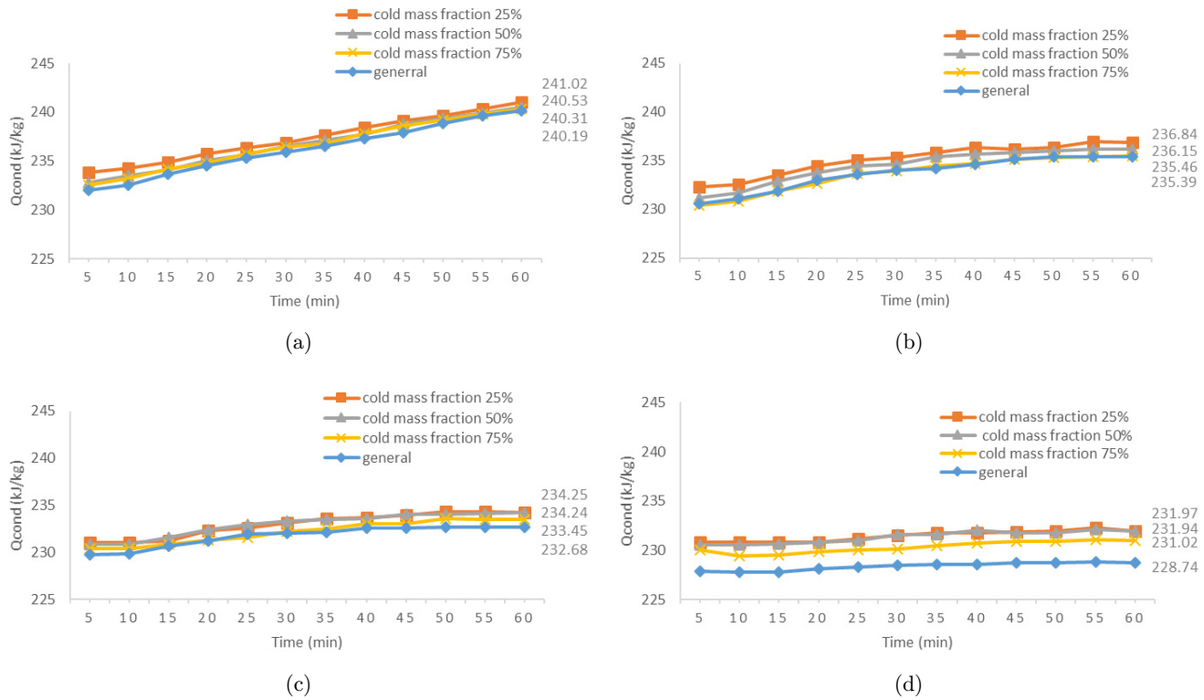

Fig. 8. Similarities between heat rejections for the VCR system using vortex tube cooling: (a) Load of 25%, (b) load of 50%, (c) load of 75% and (d) load of 100%.

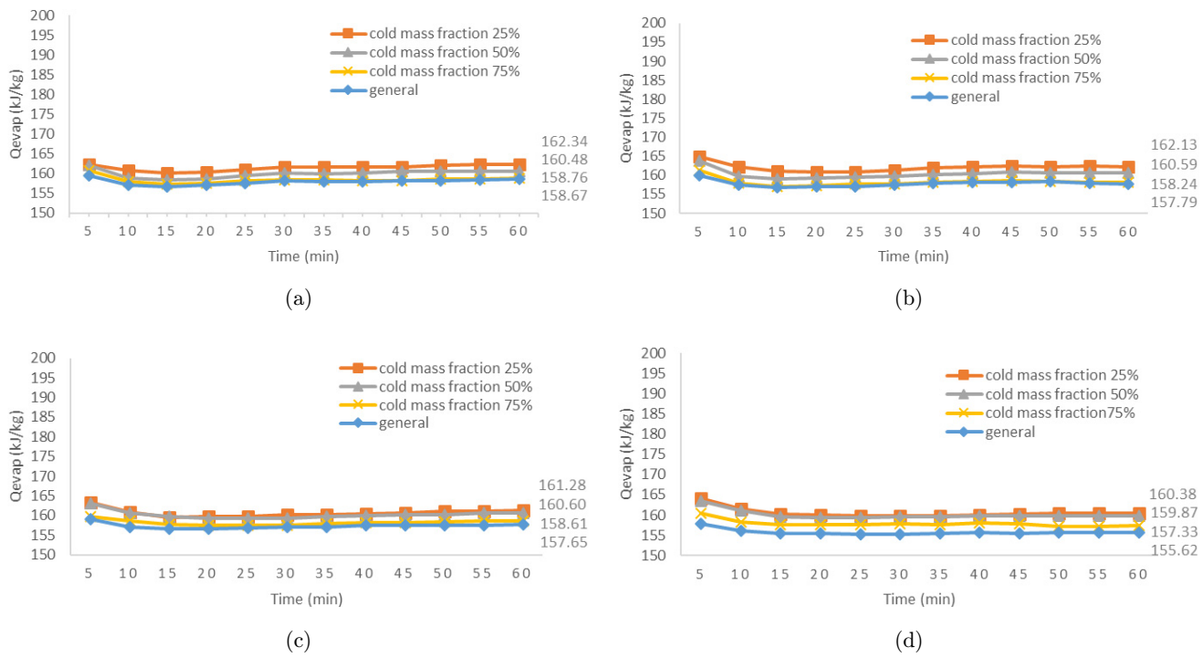

Fig. 9. Similarities between refrigerating effects in the VCR system using vortex tube cooling: (a) Load of 25%, (b) load of 50%, (c) load of 75% and (d) load of 100%.

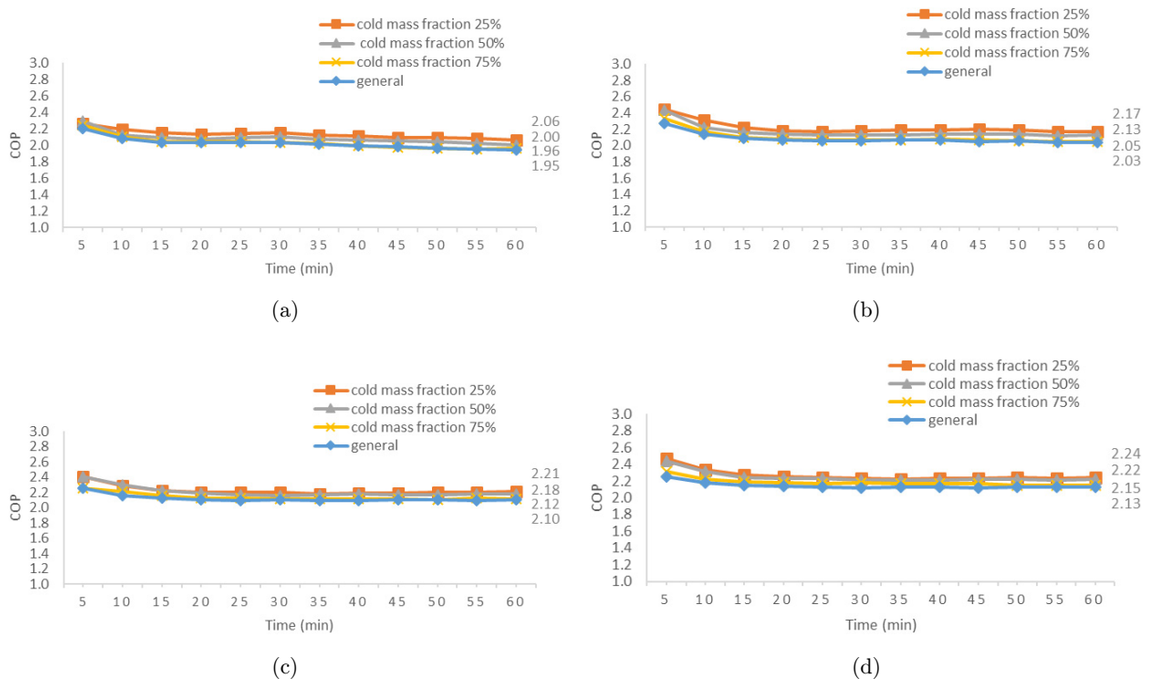

Fig. 10. Similarities between the COPs of the VCR system with vortex tube cooling: (a) Load of 25%, (b) load of 50%, (c) load of 75% and (d) load of 100%.

obvious that the cold mass fraction of 25% [shown in Fig. 9(a)] possesses the highest refrigerating effect of 2.31%. With the refrigerating effect increased by 1.14%, the cold mass fraction of 50% follows. Lastly, the effect for cold mass fraction of 75% increased only slightly by 0.05%. Further, for the load of 100% [shown in Fig. 9(d)], the cold mass fraction of 25% has the greatest refrigerating effect of 3.05% compared to conventional systems, with the cold mass fraction of 50% following, in which the refrigerating effect rose by 2.73%, and the cold mass fraction of 75% being the last, where the heat rejection boosted up by 1.09%. The trend of increasing refrigerating effect is obviously the same as for heat rejection. The cold mass fraction of 25% has the maximum value, subsequently followed by those of 50% and 75%, respectively. It seems apparent that the heat rejection of the system surges, causing an elevated refrigerating effect.

3.3. *Similarities between the coefficients of performance for the vapor compression refrigeration system*

As can be seen in Fig. 10, the efficiency coefficient is determined using Eq. (4), for different loads (25%, 50%, 75% and 100%) and separate cold mass fractions (25%, 50% and 75%). Compared to conventional vapor compression systems, the vapor compression refrigeration system using vortex cooling appears to have a higher coefficient of performance.

As shown in the results in Fig. 10(d), the best COP was achieved with a cold mass fraction of 25%, which was 5.16% higher than that for conventional systems, followed by that for a cold mass fraction of 50%, with a boost of 4.22%. Lastly, the COP for a cold mass fraction of 75% rose only slightly by 0.93%. It is apparent that the performance will have similar features. The highest value was for the cold mass fraction of 25%, followed by those of 50% and 75%, respectively. Thus, it is observable that the refrigerating effect of system is amplified, causing enhanced coefficient of performance.

3.4. *Power consumption comparison for the vapor compression refrigeration system*

Figure 11 shows the power consumptions for the vapor compression refrigeration system, at different

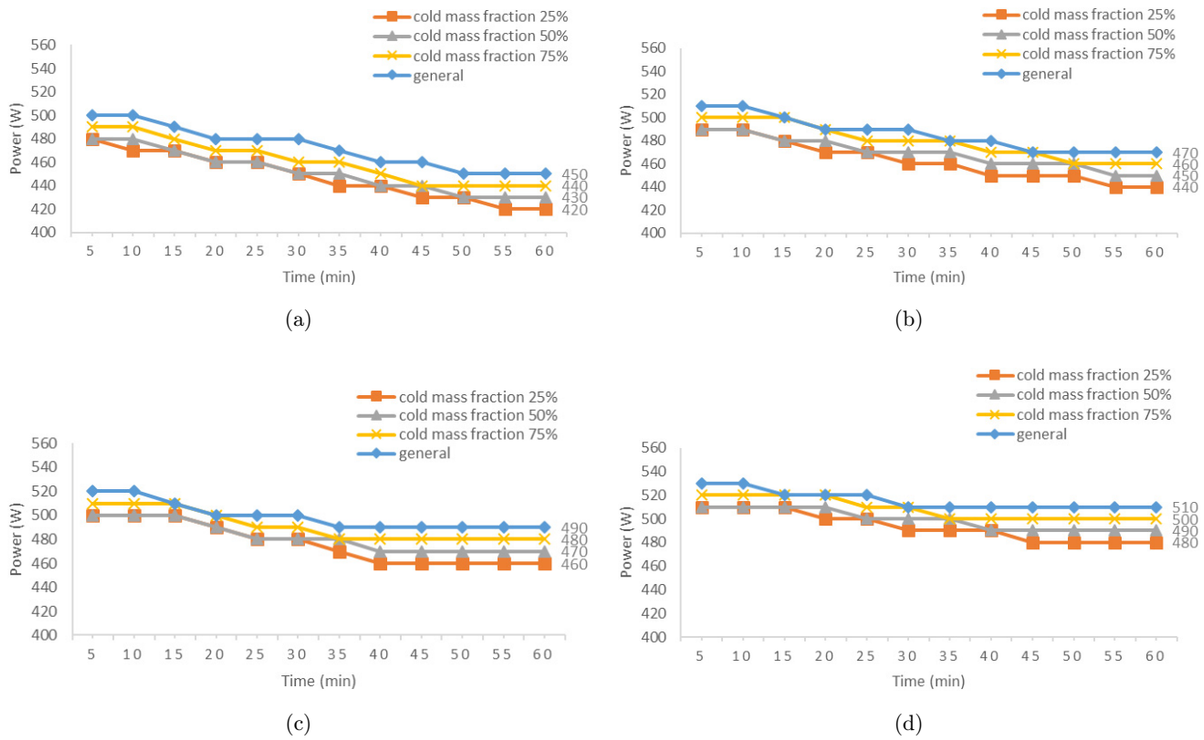

Fig. 11. Divergence between power consumptions with vortex tube cooling in the VCR system: (a) Load of 25%, (b) load of 50%, (c) load of 75% and (d) load of 100%.

loads (25%, 50%, 75% and 100%) and distinctive cold mass fractions (25%, 50% and 75%). Compared to a conventional system, the vortex system obviously has lower energy consumption.

Figure 11 illustrates a comparison of power consumption at various loads for the vapor compression refrigeration system with vortex tube cooling. Compared to a conventional system, the vortex system uses less energy. The cold mass fraction of 25% has the least power consumption when compared at various loads (25%, 50%, 75% and 100%), which reduced by 4.36% compared to conventional systems. The cold mass fraction of 50% was the next, at which power use was lowered by 3.23%. Lastly, there is only 1.45% reduction for the case of cold mass fraction of 75%. It is apparent that the heat is relocated prior to going into the condenser. Accordingly, the working pressure (high pressure) of the condenser is reduced, causing less compression work.

Enhanced heat rejection is possible using this system. Some of the heat is removed in the heat exchanger before going into the condenser. The air from the vortex tube moving inside the heat exchanger is cooler than the temperature of the immediate surroundings. The refrigerant at the condenser outlet has a lower temperature as well. More refrigerant moves through the expansion valve because it is subcooled. Consequently, there is an enhanced refrigerating effect of the system, causing better coefficient of performance.

4. Conclusions

For performance enhancement in a vapor compression refrigeration system, this experimental investigation concentrates on the use of a vortex tube. Following are the significant experimental findings of this study:

(1) The highest value for heat rejection is at 25% load, followed by those at 50%, 75% and 100% loads, respectively. Heat rejection is enhanced by the system. When compared to a conventional vapor compression refrigeration system, the vapor compression refrigeration system using vortex tube cooling enables better heat rejection.

(2) The highest refrigeration effect is at 25% cold mass fraction, followed by those at cold mass fractions of 50% and 75%, respectively. In comparison with the vapor compression refrigeration system using vortex tube cooling, a conventional vapor compression refrigeration system's refrigeration effect is lower.
(3) The highest efficiency with a coefficient of performance of 2.24 is possible when using the vapor compression refrigeration system with vortex tube cooling at 25% cold mass fraction and 100% load.
(4) Compared to conventional systems, power consumption at 25% cold mass fraction is the lowest, followed by those at cold mass fractions of 50% and 75%.

Acknowledgments

The authors are thankful to RCSEE, Rajamangala University of Technology Rattanakosin (RMUTR), for its financial and resource support, to Rajamangala University of Technology Phra Nakhon (RMUTP) for supporting with the materials used in the experiment and resource support, to the Thailand Science Research and Innovation and Thailand Government Budget Grant provided financial support for this work.

References

1. A. Kumar, Vivekanand and S. Subudhi, Cooling and dehumidification using vortex tube, *Appl. Therm. Eng.* **122** (2017) 181–193.
2. G. J. Ranque, Experiments on expansion in a vortex with simultaneous exhaust of hot and cold air, *J. Phys. Radium (Paris)* **4** (1933) 112–114.
3. R. Hilsch, The use of the expansion of gases in a centrifugal field as cooling process, *Rev. Sci. Instrum.* **18** (1947) 108–113.
4. S. Subudhi and M. Sen, Review of Ranque–Hilsch vortex tube experiments using air, *Renew. Sustain. Energy Rev.* **52** (2015) 172–178.
5. T. Bornare, A. Badgujar and P. Natu, Vortex tube refrigeration system based on compressed air, *Int. J. Mech. Eng. Technol.* **6** (2015) 97–102.
6. Y. T. Wu, Y. Ding, Y. B. Ji, C. F. Ma and M. C. Ge, Modification and experimental research on vortex tube, *Int. J. Refrig.* **30** (2007) 1042–1049.
7. V. Kirmaci, Exergy analysis and performance of a counter flow Ranque-Hilsch vortex tube having various nozzle numbers at different inlet pressures of oxygen and air, *Int. J. Refrig.* **32** (2009) 1626–1633.
8. B. Markal, O. Aydın and M. Avcı, An experimental study on the effect of the valve angle of counter-flow Ranque–Hilsch vortex tubes on thermal energy separation, *Exp. Therm. Fluid Sci.* **34** (2010) 966–971.
9. S. Eiamsa-ard, Experimental investigation of energy separation in a counter-flow Ranque–Hilsch vortex tube with multiple inlet snail entries, *Int. Commun. Heat Mass Transf.* **37** (2010) 637–643.
10. C. Park, H. Lee, Y. Hwang and R. Radermacher, Recent advances in vapor compression cycle technologies, *Int. J. Refrig.* **60** (2015) 118–134.
11. H. Cho, H. Lee and C. Park, Performance characteristics of an automobile air conditioning system with internal heat exchanger using refrigerant R1234yf, *Appl. Therm. Eng.* **61** (2013) 563–569.
12. G. Pottker and P. Hrnjak, Experimental investigation of the effect of condenser subcooling in R134a and R1234yf air conditioning systems with and without internal heat exchanger, *Int. J. Refrig.* **50** (2015) 104–113.
13. G. Pottker and P. Hrnjak, Effect of condenser subcooling on the performance of vapor compression system, *Int. J. Refrig.* **50** (2015) 156–164.
14. E. Hajidavalloo and H. Eghtedari, Performance improvement of air-cooled refrigeration system by using an evaporatively cooled air condenser, *Int. J. Refrig.* **33** (2010) 982–988.
15. A. Ghute and V. M. Kulkarni, Experimental study of variation in performance parameters of VCR system with & without subcooling of refrigerant by thermoelectric Peltier cooling module, *Int. J. Mech. Eng. Technol.* **10** (2019) 1662–1670.
16. B. A. Qureshi, M. Inam, M. A. Antar and S. M. Zubair, Experimental energetic analysis of a vapor compression refrigeration system with dedicated mechanical sub-cooling, *Appl. Energy* **102** (2013) 1035–1041.
17. P. A. Domanski and D. A. Didion, Evaluation of suction-line/liquid-line heat exchange in the refrigeration cycle, *Int. J. Refrig.* **17** (1994) 487–493.
18. D. Boewe, J. Yin, Y. C. Park, C. W. Bullard and P. S. Hrnjak, The role of suction line heat exchanger in transcritical R744 mobile A/C systems, SAE Technical Paper No. 1999-01-0583 (1999).
19. X. Z. Li, J. Che and P. Hrnjak, Experimentally verified potential to improve performance of the R134a systems by internal heat exchanger, *Proc. SAE 2004 World Congr. & Exhibition* (2004).
20. J. L. Hermes, Alternative evaluation of liquid-to-suction heat exchange in the refrigeration cycle, *Int. J. Refrig.* **36** (2013) 2119–2127.

21. W. Naksanee and R. Prommas, An experimental investigation on the efficiency of snail entry in vortex tube fed low inlet air pressure to reduce temperature of low pressure air, *Int. J. Heat Technol.* **36** (2018) 1223–1232.
22. R. Prommas, S. Phiraphat and P. Rattanadecho, Energy and exergy analyses of PV roof solar collector, *Int. J. Heat Technol.* **37** (2019) 303–312.
23. D. Nonthiworawong, P. Rattanadecho and R. Prommas, Energy and exergy analysis of low-cooling in building by using light-vent pipe, *Sci. Technol. Asia* **24** (2019) 41–53.
24. C. Phongthanachote, P. Rattanadecho, C. Corn-arch and R. Prommas, Animation and computer games design to build awareness of energy conservation, *Sci. Technol. Asia* **24** (2019) 21–29.
25. P. Rattanapunt, C. Corn-arch, S. Sungsoontorn and R. Prommas, A study of characteristics of palm oil biomass by using torrefaction process, *Sci. Technol. Asia* **23** (2018) 23–31.
26. U. Sriphan, P. Kerdchang, R. Prommas and T. Bunnang, Coefficient of performance of battery running and charging by magnet generator Bedini, *J. Electrochem. Energy Convers. Storage* **15** (2018) 041002.
27. S. Phiraphata, R. Prommas and W. Puangsombut, Experimental study of natural convection in PV roof solar collector, *Int. Commun. Heat Mass Transf.* **89** (2017) 31–38.
28. C. Chokpanyasuwan, K. Hussaro, T. Bunnag and R. Prommas, Artificial intelligence for load management based on load shifting in the textile industry, *Int. J. Eng. Technol.* **7** (2015) 350–367.
29. C. Chokpanyasuwan, K. Hussaro, T. Bunnag and R. Prommas, Bee algorithm optimization for load management based on load shifting in the textile industry, *WSEAS Trans. Power Syst.* **10** (2015) 215–229.
30. C. Chokpanyasuwan, T. Bunnag and R. Prommas, Ant colony optimization for load management based on load shifting in the textile industry, *Am. J. Appl. Sci.* **12** (2015) 142–154.
31. R. Prommas and T. Rungsakthaweekul, Effect of microwave curing conditions on high strength concrete properties, *Energy Procedia* **56** (2014) 26–34.
32. R. Prommas, P. Rattanadecho and W. Jindarat, Energy and exergy analyses in drying process of non-hygroscopic porous packed bed using a combined multi-feed microwave-convective air and continuous belt system (CMCB), *Int. Commun. Heat Mass Transf.* **39** (2012) 242–250.
33. R. Prommas, Theoretical and experimental study of heat and mass transfer mechanism during convective drying of multi-layered porous packed bed, *Int. Commun. Heat Mass Transf.* **38** (2011) 900–905.
34. R. Prommas, P. Keangin and P. Rattanadecho, Energy and exergy analyses in convective drying process of multi-layered porous packed bed, *Int. Commun. Heat Mass Transf.* **37** (2010) 1106–1114.
35. R. Prommas, P. Rattanadecho and D. Cholaseuk, Energy and exergy analyses in drying process of porous media using hot air, *Int. Commun. Heat Mass Transf.* **37** (2010) 372–378.